Received 27 February 2021; revised 31 March 2021; accepted 15 April 2021. Date of publication 22 April 2021; date of current version 30 April 2021.

Digital Object Identifier 10.1109/OJCOMS.2021.3075081

Cooperative Non-Orthogonal Multiple Access for Beyond 5G Networks

ABBAS AHMED, ZEYAD ELSARAF, FAHEEM A. KHAN (Member, IEEE), AND QASIM ZEESHAN AHMED

Department of Engineering and Technology, University of Huddersfield, Huddersfield HD1 3DH, U.K.

CORRESPONDING AUTHOR: Q. Z. AHMED (e-mail: q.ahmed@hud.ac.uk)

This work was supported by the Proof of Concept funding from University of Huddersfield, U.K.

ABSTRACT In the beyond 5G networks, extraordinary demands for data rates and capacity are to be met. A possible candidate to address these challenges is Non-Orthogonal Multiple Access (NOMA) technique, which leads to higher diversity gains and massive connectivity. One caveat of NOMA is the increased receiver complexity to nullify the Inter User Interference (IUI) through Successive Interference Cancellation (SIC). In this paper, a cooperative relaying scheme is employed to improve the overall diversity gain and data rates of the NOMA system. Extrinsic Information Transfer (EXIT) charts are employed to examine the cooperative NOMA system's user fairness as well as its performance while implementing the IRregular Convolutional Code (IRCC). The EXIT chart using IRCC evaluates the convergence analysis for the proposed system. Furthermore, the implementation of EXIT charts for optimization convergence is exploited by using power optimization and the SIC for the joint rate to evaluate the fairness of the system. Simulation results shows that cooperative NOMA helps to achieve higher diversity gain and improved data rate for the cooperative NOMA system.

INDEX TERMS Cooperative communications, extrinsic information transfer, multiple access, non-orthogonal multiple access, orthogonal multiple access, successive interference cancellation.

I. INTRODUCTION

THE EXPONENTIAL increase in Internet of Things (IoT) networks, wireless services, and applications in recent years has led to several challenging needs for the Beyond 5G networks, which is indicated by the anticipation of nearly a thousandfold increase in data traffic, much lower latency, massive connectivity, and higher spectral efficiency [1]–[8]. To fulfil the diverse requirements of the Beyond 5G, several key technologies such as millimeter Wave (mmWave), massive Multiple-Input Multiple-Output (MIMO), and dynamic spectrum sharing have been considered yet the present cellular networks still employ Orthogonal Multiple Access (OMA) schemes where users are separated in time, frequency, code or space domain. It is well known that the OMA is an inherently inefficient way of multiple access as it limits the number of users to be served based on orthogonal resources available [3], [9]–[14].

Non-Orthogonal Multiple Access (NOMA) has recently been considered as a key technology for Beyond 5G networks where multiple users are served using the same time and frequency resources, leading to a significant increase in spectrum efficiency [4], [15]–[22]. NOMA schemes are mainly divided in two categories: Code Domain NOMA (CD-NOMA) [3], [22], [23] and Power Domain NOMA (PD-NOMA) [3], [9], [23], [24]. CD-NOMA achieves the non-orthogonal multiple access by assigning users unique spreading codes [3], [22], [23]. The code words are sparse in design to allow for a higher number of unique codes to avoid inter user interference (IUI) [3], [22], [23]. In PD-NOMA, users share time, frequency, or code slot by operating at varying power levels for every available resource [3], [9], [23]. The powers levels are allocated before transmission using classical NOMA principle [23], [25], where users with worse channel conditions are allocated higher power levels and ones with better channel conditions are allocated less power levels. Such power allocation results in an increased receiver complexity as Successive Interference Cancellation (SIC) is needed at the receiver [4]. SIC acts as the reception mechanism for users with superior channel conditions [3], [4], [9]. The detection is carried out by performing the subtraction of

the stronger signal from the received signal to successfully extract the correct data for the user [23], [26].

One drawback of PD-NOMA scheme is its favoring of users with worse channel conditions which provides weak users with nearly all the available transmission power or as much as possible, leaving users with stronger channels with almost no power to serve their needs in some extreme cases [1], [27], [28], limiting individual user performance. Combining cooperative relaying with PD-NOMA promises to alleviate many of NOMAs issues with significant improvement in diversity gains leading to superior reception reliability and user fairness for the users with stronger channels [29], [30]. The main point to note is exploiting the properties of the SIC process, namely the availability of other users' data at one user while combining it with cooperative relaying to achieve the expected performance [27].

Several cooperative NOMA schemes have been considered in the literature from various perspectives [31]. For example, in [32] the effect of relay selection (RS) on the performance of cooperative NOMA is considered. A two-stage RS strategy is used to obtain the minimal outage probability considering different relay selection schemes while realizing the maximum possible diversity gain. In [31], three typical structures of cooperative relaying based NOMA, e.g., uplink, downlink and composite structure have been investigated. A hybrid power allocation scheme is proposed that has lower computational complexity and requires lesser signalling overhead at the cost of minimal degradation in the sum rate. In [33], a cooperative NOMA transmission scheme is studied by considering the prior information by some users in NOMA system about the other users' messages. Results are shown to achieve the superior performance for the proposed cooperative NOMA scheme.

In [34], a cooperative NOMA relaying scheme is proposed where the two sources communicate with their destinations via a common relay in the same frequency band. The relay in this scheme sends a NOMA based superposition coded composite signal to the destinations after receiving the symbols by both sources with different allocated powers. The proposed protocol is demonstrated to be effective with regard to ergodic sum capacity by considering perfect as well as imperfect SIC.

In [35], cognitive radio (CR) NOMA schemes are employed for efficient utilization of wireless spectrum. This work has considered three different cognitive NOMA schemes based on underlay, overlay, and CR NOMA networks. Cooperative relaying strategies are proposed to address inter- and intra-network interferences in CR NOMA networks. It is shown that for each CR NOMA scheme, cooperative relaying strategies lead to much lower outage probabilities. In [36], multicast cognitive radio NOMA (MCR-NOMA) networks are investigated and dynamic cooperative schemes are proposed. The performance of primary and secondary networks is shown to be improved by using the multicast secondary users as relays. Various scheduling schemes involving secondary users for the cooperative MCR-NOMA are considered. It is shown that superior performance is achieved in terms of outage probability and diversity order for both networks.

In [37], a two-user, FD cooperative NOMA system is considered. The information transmission to the user with weak channel is carried out with the help of a dedicated FD relay. The achievable outage probability and ergodic sum capacity is investigated for both users considering imperfect self-interference cancellation. It is demonstrated that the proposed FD cooperative NOMA system attains superior performance compared to half-duplex system. In [38], a FD multi-user NOMA communication system is investigated with regard to the optimization of received signal-to-interference-plus-noise ratio (SINR) per unit power. A game-theoretic approach is adopted to combat the Co-Channel Interference (CCI), and users clustering algorithms are proposed. The original non-convex power normalized (PN) SINR problem is transformed into an equivalent subtractive-form problem. To obtain the optimal power allocation, an iterative algorithm is employed. It is shown that the considered FD-NOMA system has superior performance over HD-NOMA and FD-OMA systems considering the channel conditions, Self-Interference (SI) and CCI.

User pairing has recently attracted significant attention in mitigating the complexity of cooperative NOMA systems and attaining the capacity gain. In [23], two-user pairing is utilized to demonstrate that higher gain on sum rate can be achieved for user pairs with substantial difference in channel conditions in a NOMA system in comparison to OMA based systems. In [39], multiple similar gain users in NOMA system are paired to a single far user in a non-overlapping way to achieve efficient spectrum utilization of unpaired users. It is shown that capacity gain of NOMA system is increased substantially using this scheme compared to the usual NOMA as well as OMA systems. In [40], user pairing with non-uniform distribution of users in a NOMA system is investigated. A time sharing based strategy is used where user from lesser dense area are paired with users from denser area on time sharing basis. It is shown that time sharing NOMA scheme has superior performance compared to cooperative NOMA and OMA schemes.

In this paper, we consider a cooperative PD-NOMA system where a base station is serving several near users and a single far user in the same frequency band at the same time and all users have single antenna each. We investigate the performance of cooperative PD-NOMA system by exploiting the concept of the EXIT chart. Moreover, we implement IRregular Convolutional Code (IRCC) to evaluate the EXIT chart analysis for the cooperative NOMA system. Whilst EXIT chart analysis is implemented in [41] to investigate the uplink NOMA performance by applying power optimization and SIC, the EXIT chart analysis has not been applied in the cooperative NOMA system to the best of our knowledge. Also, the EXIT chart based approach has not been used to evaluate the convergence

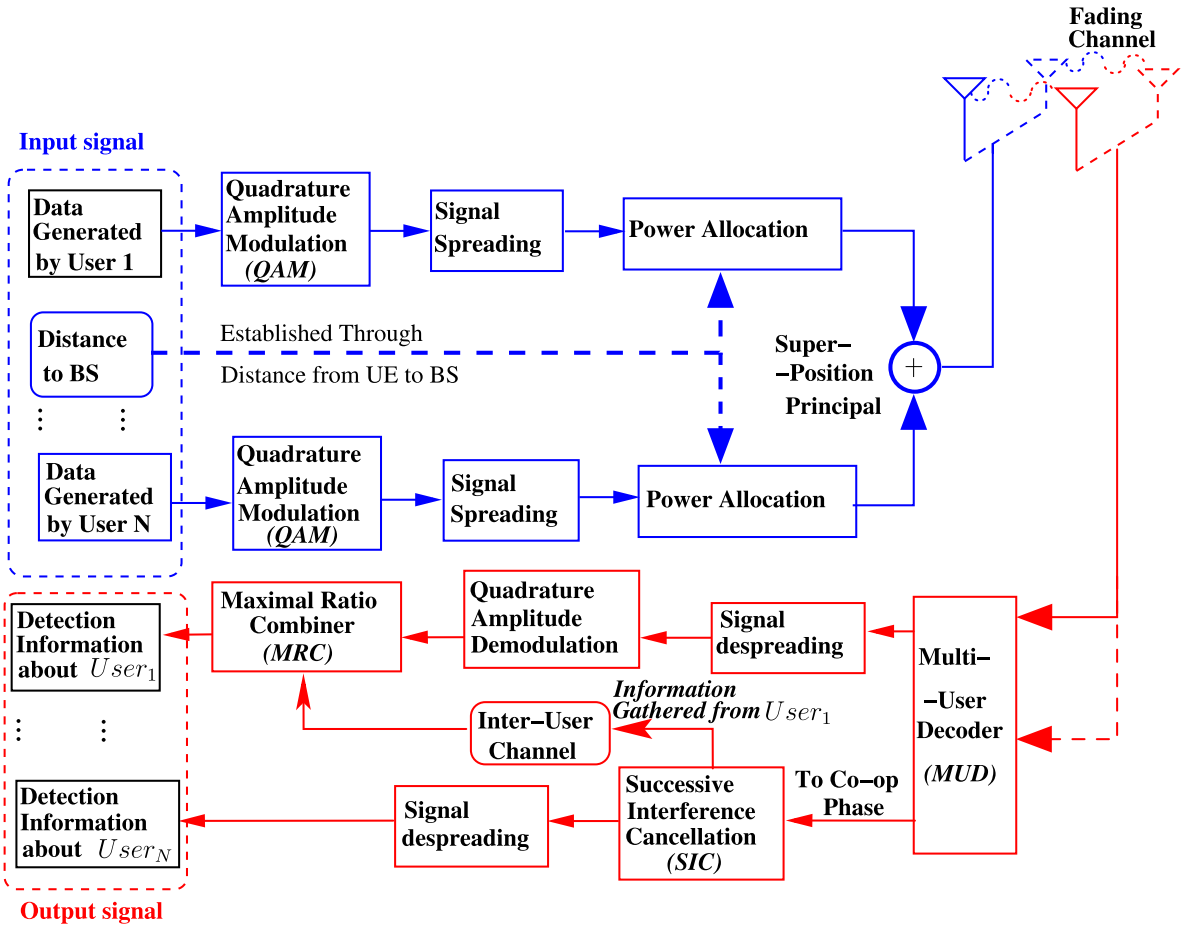

FIGURE 1. Proposed NOMA System Model.

behavior of cooperative NOMA system in the previous works.

The main contributions of this paper are as follows:

- We have implemented a PD-NOMA two-phase cooperative relaying scheme and evaluated the data rate and throughput of the cooperative NOMA system.
- We have evaluated the performance based on the power allocation with regard to Far User (FU) and the Near User (NU) data rates.
- We have evaluated Multi User Detector (MUD) in NOMA system through the EXIT chart by using the IRregular Convolutional Code (IRCC).
- Performance evaluation of MUD is carried out regarding he Bit Error Rate (BER) versus Signal to Noise Ratio (SNR) by comparing the system performance with the channel capacity.
- We have investigated the normalization throughput by utilizing the concept of MUD in NOMA system.
- We have demonstrated that joint alphabet MUD model achieves a higher achievable capacity than the single user in the cooperative NOMA scenarios.

The paper consists of the following sections: The proposed system model is discussed in Section II, while in Section III the data rates are derived initially for each user while considering the IUI and independent fading which occur in the NOMA system independently. The throughput analysis is then carried out for the NOMA system and finally, the EXIT charts analysis is carried out, where we have analyzed the diversity gains, normalization throughput, and complexity in the MUD decoder. Furthermore, in Section IV simulation results are discussed. Finally, the conclusion is presented in Section V.

II. SYSTEM MODEL

Fig. 1 shows the system model of the proposed cooperative NOMA system. The user data is sent to the Quadrature Amplitude Modulator (QAM), where the information bits are mapped. These bits are spread by the predesigned codewords and allocated a power according to NOMA principles as mentioned in [4], [23]. This information is transmitted to the receiver through a fading channel. The Multi-User Detector (MUD) at the receiver side caters for interference caused by the channel. The signal is despread as the predesigned code

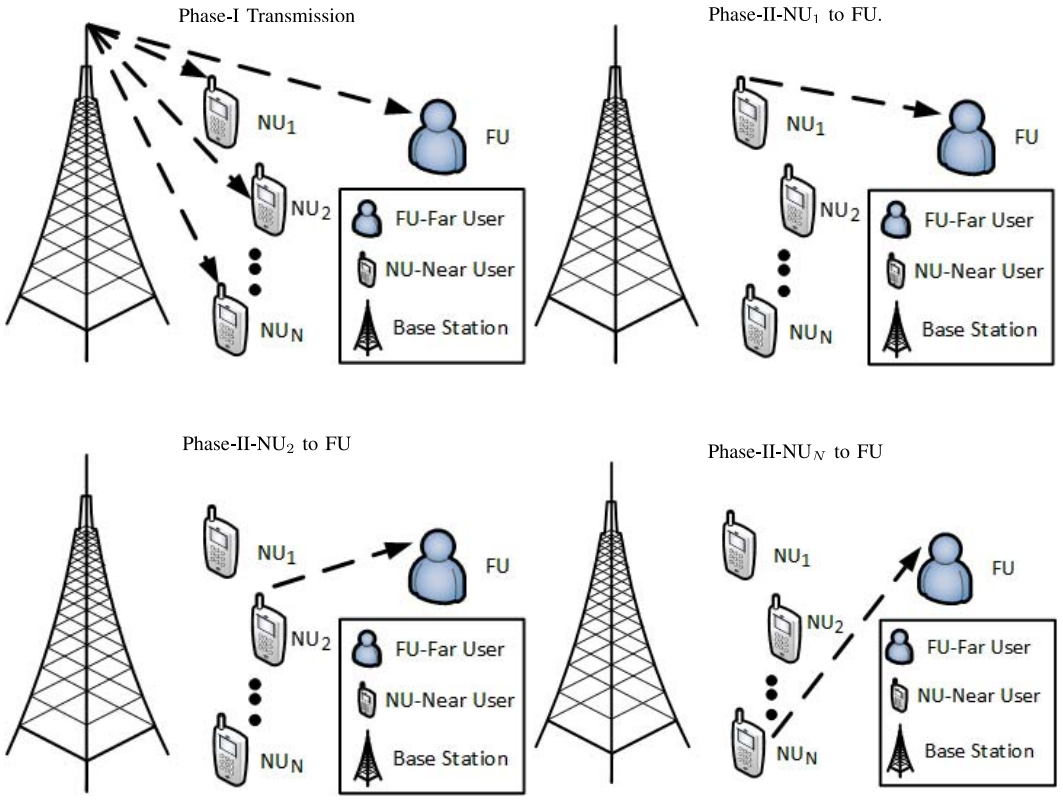

FIGURE 2. Block Diagram for Cooperative NOMA system where transmission between *N* near users and a far user is shown.

is known at the receiver. Finally, Maximal Ratio Combining (MRC) is employed after demodulation of the user bits as shown in Fig. 1.

Cooperative communication for NOMA is illustrated in Fig. 2. From the figure, it can be observed that two different types of users are present. There are N number of Near Users (NU)s which are located near the BS and a Far User (FU) present in the system. Phase-I and Phase-II are the two communication phases. Each communication phase is described in detail as follows.

A. PHASE-I

The BS broadcasts the signal to all the N-NUs and the FU in Phase-I as shown in Fig. 2. This signal consists of superimposed sigal of N-NUs according to the principles of NOMA. The n^{th} NU user signal is given as:

$$r_{n,1} = h_{n,1}x + \sqrt{P_{FU}}h_{n,1}x_{FU} + w_{n,1}, \tag{1}$$

where the FU power is allocated as P_{FU}. x represents composite signal by containing all n^{th}-NU users' messages such that $x = \sqrt{P}_1x_1 + \sqrt{P}_2x_2 + \cdots + \sqrt{P}_Nx_N$ and the Additive White Gaussian Noise (AWGN) is expressed as $w_{n,1}$ for each channel during the Phase-I. $h_{n,1}$ is the channel experienced by every user which in this case is modeled as an independent Rayleigh fading. Power level allocation is carried out by determining the distance of the n-th user from the BS [23], [29]. In our power allocation, the strongest user is allocated the minimum power, whereas the weakest user is allocated the maximum power. Furthermore, the channel conditions for NOMA model are expressed by [26]:

$$\left|h_{FU,1}\right|^2 < \left|h_{1,1}\right|^2 < \left|h_{2,1}\right|^2 < \cdots < \left|h_{N,1}\right|^2, \tag{2}$$

which are accordingly expressed as:

$$P_{FU} > P_1 > P_2 > \cdots > P_N, \tag{3}$$

and

$$P_{FU} + \sum_{n=1}^{N} P_n = 1. \tag{4}$$

B. PHASE-II

In Fig. 2, the Phase-II is illustrated. This phase is divided intro N time slots. The N users utilize their assigned time slot to relay and broadcast the data to the FU. Every transmission is done separately, possessing different time slots to avoid IUI. At the beginning of the Phase-II, the n^{th}NU will wait and then broadcasts a signal comprised of the data of the FU in the n-th time slot. After all the cooperative relaying is completed, the signal received by the FU from the n-th relay will be expressed as:

$$r_{n,2} = \sqrt{P_{n,2}}h_{n,2}x_{FU} + w_{n,2}, n = 1, 2, \ldots, N, \tag{5}$$

where $P_{n,2}$ is the power allocated by the n^{th} user, $h_{n,2}$ represents the cooperative signals passing through inter-user channels where all channel experience independent Rayleigh fading and $w_{n,2}$ represents the AWGN noise.

III. PERFORMANCE ANALYSIS

We assume that ideal detection takes place during both these phases. The proposed cooperative NOMA performance is measured in terms of system throughput and each user data rate.

A. DATA RATE

After the completion of Phase-I, the n-th NU will apply the SIC principles and the user data rate is expressed as:

$$R_n = \log_2\left(1 + \frac{P_n\left|h_{n,1}\right|^2}{\sum_{j=n+1}^{N} P_j\left|h_{n,1}\right|^2 + N_{0_{n,1}}}\right), \tag{6}$$

where $N_{0_{n,1}}$ is equivalent to the noise variance at the completion of Phase-I. This expression is used for calculating the data rate of the n-th NU.

It can be observed from Fig. 2 that by adopting MRC at the receiver, the data rate for the FU after completing the second phase will be expressed as:

$$R_{FU} = \log_2\left(1 + \frac{P_{FU}\left|h_{FU,1}\right|^2}{\sum_{n=1}^{N} P_n\left|h_{FU,1}\right|^2 + N_{0_{FU_1}}} + \frac{1}{N}\sum_{n=1}^{N}\frac{P_{n,2}\left|h_{n,2}\right|^2}{N_{0_{FU_2}}}\right). \tag{7}$$

Equation (7) represents the data rate of the FU. It should be noted that the data rate of FU will be dependent upon summation of two slots. However, in the second slot as the data is received N times and then MRC is used, it is therefore normalized by N.

B. THROUGHPUT

Throughput of the system is defined as the aggregate data rates experienced by each user. As it is a main performance metric and also enable us to measure the overall efficiency of the cooperative NOMA system. The throughput of the system is represented as:

$$S = \sum_{n=1}^{N} R_n + R_{FU}. \tag{8}$$

C. EXIT CHART

Iterative decoding is used in the EXIT charts to inspect and monitor the convergence analysis of the system [42]–[45]. EXIT charts help us avoid Monte Carlo Simulations, as low BER can be predicted easily at a given SNR using these charts [45], [46]. EXIT charts exchanges the information between the MUD module by changing the conditions of the channel as shown in Fig. 3. The MUD module also calculates the joint alphabet probability. These probabilities can be calculated offline at the BS and the user. The upper left-hand side of Fig. 3 represents the transmission box and the lower half represents the reception box, which is similar to the one shown in Fig. 1 of our proposed cooperative NOMA model. This is achieved by utilizing the fair selection of the codewords in parallel with the predetermined values of the interleavers of our system. Generally EXIT chart has a trajectory, inner and outer curves. Interleavers are employed to simulate the EXIT charts. Ideally, when interleavers of smaller length are employed for any system, the trajectory will not perfectly match to the inner and outer curves of the EXIT chart [42], [44], [47]. Therefore, interleavers having long lengths are employed.

As we have N NU users and 1 FU, the channel encoder as shown in Fig. 3 uses a Recursive Systematic Convolution (RSC) codes. This information is forwarded to the signal spreader which employs spread spectrum principles to encode this information [47], [48]. This information is passed to the interleavers and then mapped by the signal mapper and transmitted over the antenna. At the receiver side, the mapped signal information of all the users is achieved and the MUD performs the Log Likelihood Ratio (LLR). The extrinsic LLR of the n^{th} user's output bit from the MUD is evaluated as:

$$L_{ex}\left(i^{(n)}\right) = \ln\frac{\sum_{r\in\upsilon(0)} P(v|r)P(r)}{\sum_{Y\in\upsilon(1)} P(v|r)P(r)} - L_{apr}\left(i^{(n)}\right), \tag{9}$$

where $v \in \{0, 1\}$. Hence, the *a priori* LLR of the n^{th} user is denoted by $L_{apr}(i^{(n)})$. Please note that in MUD scenario, the initial probability of zero's and one's bits are equiprobable, thus the initial values in the soft registers are set to zeros as indicated in [44], [47] while the *a priori* symbol is denoted by $P(r)$ which represents the multi-user probability and thus the codeword is expressed as $\boldsymbol{r} = [r^{(0)}, r^{(1)}, \ldots, r^{(N)}]^T$. The channel probability with respect to the *a priori* $\boldsymbol{r}$ is expressed as $P(\boldsymbol{v}|\boldsymbol{r})$ and it evaluates the cost function of the MUD given as

$$\begin{aligned} f(\boldsymbol{r}) &= P(\boldsymbol{v}|\boldsymbol{r})P(\boldsymbol{r}) \\ &= \exp(-||\boldsymbol{v} - \boldsymbol{PHr}||^2)P(\boldsymbol{r}). \end{aligned} \tag{10}$$

where $\boldsymbol{P}$ is the allocated power, and $\boldsymbol{H}$ is the channel states of all user present in the model. Before feeding to the channel decoder the despreading is performed on *a priori* LLRs, so that the extrinsic LLRs of each user are calculated by the deinterleaving which is carried out on the user input sequence. The bit-based *a posteriori* LLRs are generated by channel decoder as shown by Fig. 3, the data is fed to the signal spreader, where more iterations are performed amongst the interleavers and the MUD as depicted in Fig. 3. After performing certain iterations 'I' among the DECoding (DEC) and MUD-Despreading/Spreading (DES), a hard decision is accomplished by the decoder, where information bits of each user is estimated at the receiver.

D. PERFORMANCE

In this section we will discuss the diversity gain, normalization throughput and the complexity involved while using the MUD in the above-mentioned NOMA model.

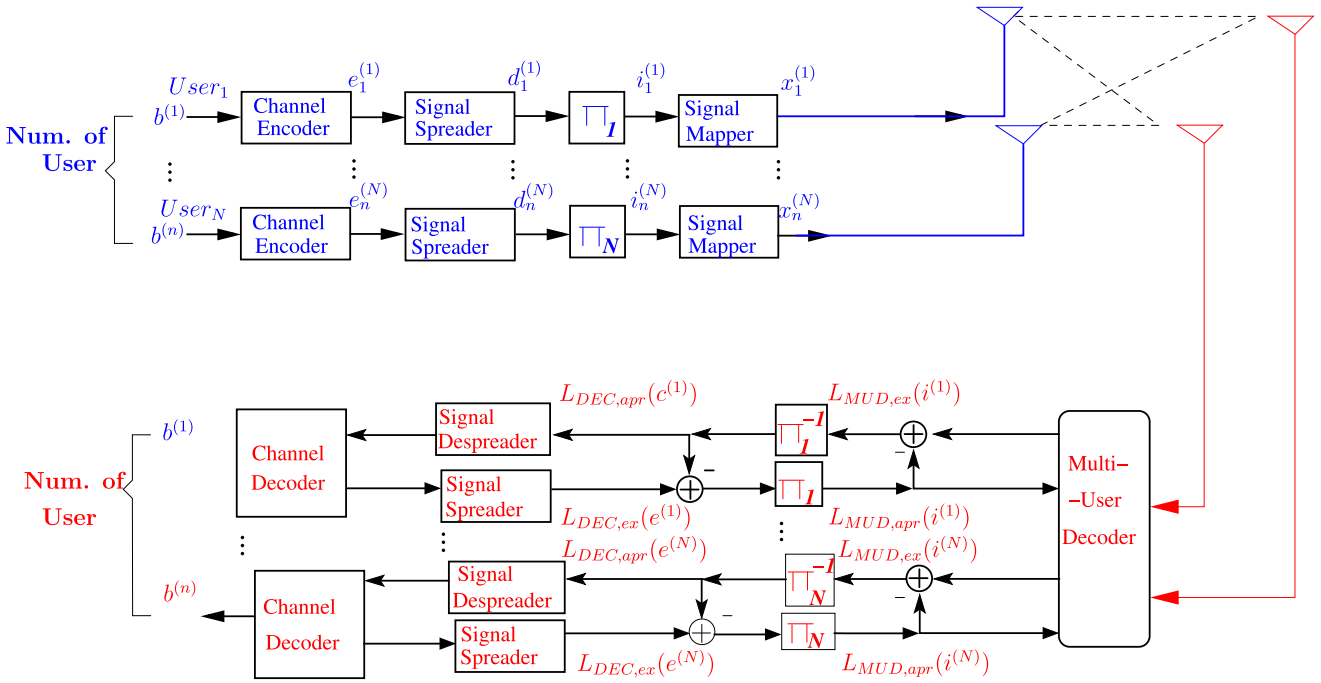

FIGURE 3. Schematic diagram of our proposed EXIT chart model.

1) DIVERSITY GAIN

It is equivalent to the number of slots assigned and is expressed as

$$\eta_{DG} = N + 1, \tag{11}$$

where N is also the number of NUs in the system. Furthermore, the system diversity gain which also determines the fair treatment of the users is expressed as

$$\eta_{IG} = N. \tag{12}$$

2) NORMALIZATION THROUGHPUT

The system normalization throughput of MUD is evaluated as

$$\textit{Normalization Throughput} = \frac{R \cdot B}{(N+1) \cdot SF} \text{ bits per channel use} \tag{13}$$

where $B = \sum_{i=0}^{N} b^{(n)}$ represents the number of bits per MUD, R represents the coding rate, and $SF = 2$ is the Spreading Factor. The inner decoder in the MUD exist of despreader and the deinterleaver and thus the system capacity can be given as

$$C = \frac{1}{N+1}\left(B - \frac{1}{2^B}\sum_{i=0}^{2^B-1} E\left[\log_2\left\{\sum_{j=0}^{2^B-1}\exp(\varphi^{(i,j)})\right\}\right]\right) \tag{14}$$

where $\varphi^{(i,j)}$ is evaluated as

$$\varphi^{(i,j)} = -||\boldsymbol{PH} + \boldsymbol{W}||^2 + ||\boldsymbol{W}||^2 \tag{15}$$

where $\boldsymbol{W}$ is the noise matrices.

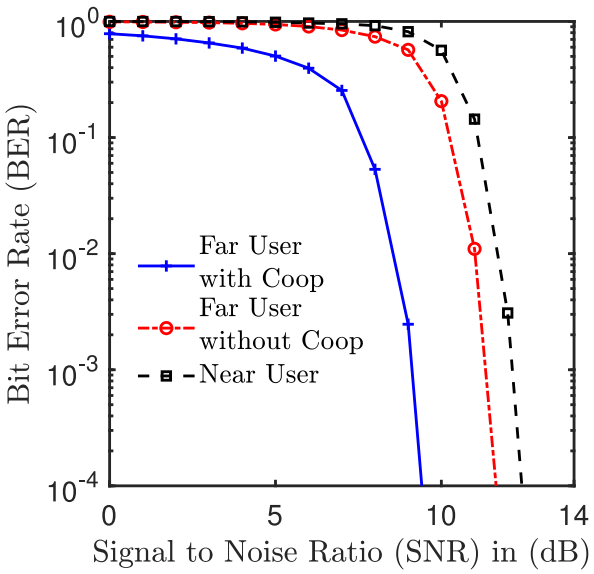

FIGURE 4. BER Performance of the NUs and FU when employing cooperative NOMA.

3) ONLINE EVALUATING COMPLEXITY IN MUD

In the MUD, the complexity arises during an iteration of the MAP detector when the Cost Function (CF) is evaluated over the number of bits evolved in the cycle. It is calculated as

$$N^{(MAP)} = \frac{\prod_{n=1}^{N} 2^{b^{(n)}}}{\sum_{n=1}^{N} b^{(n)}} \tag{16}$$

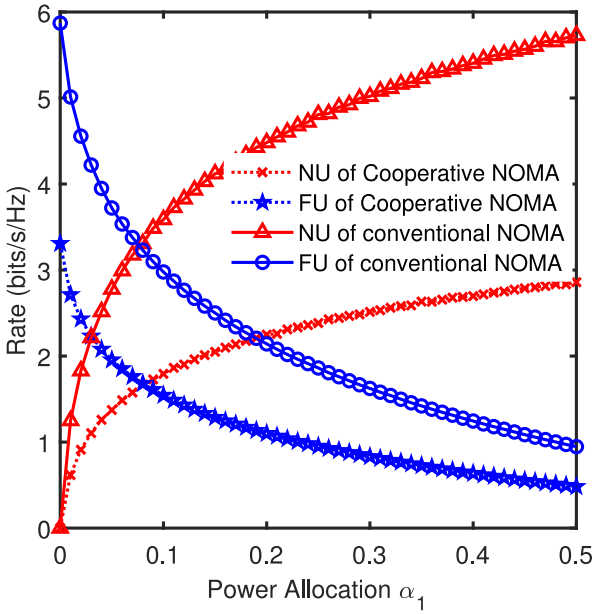

FIGURE 5. The relationship between power allocation and decoded rates in cooperative and conventional NOMA.

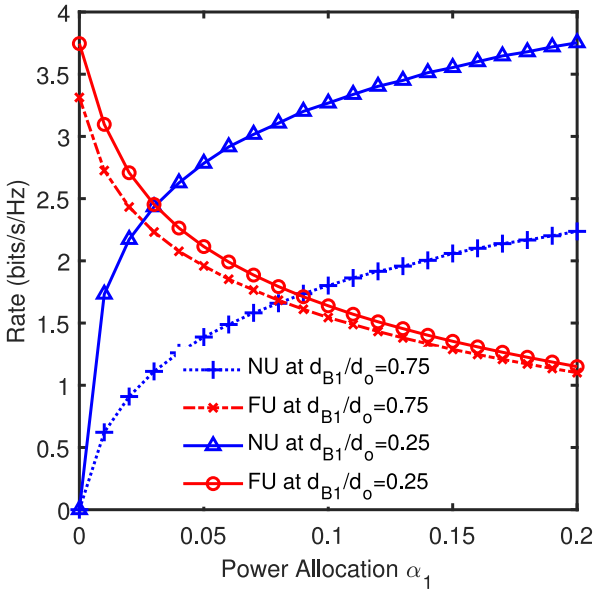

FIGURE 6. The relationship between power allocation and decoded rates when FU and NU are allocated similar power levels.

where $b^{(n)}$ is the number of bits per the codeword involved in MUD designed for the n^{th} user. Moreover, the number of users utilized in the channel, number of transmitted and number of received antennas add major contribution in the online evaluation for computing the CF, affecting the complexity in the MUD. Furthermore, the $SISO_{MUD}$ and Hard-Input Hard-Output (HIHO) are evaluated as $O(\sqrt{N^{(MAP)}_{CFEs/bits}})$ by [47].

IV. SIMULATION RESULTS

Fig. 4 shows the comparison between the conventional and cooperative NOMA when the SNR versus BER performance of the system is plotted. In this simulation only a single FU and a NU was considered. From the figure, it can be observed that the BER performance of the system improves with the improvement in SNR. From this figure, it can be observed that the performance of FU employing cooperative communication is much superior to FU that does not employ cooperation. The improvement in performance is because of diversity which is achieved due to repeated information received through the NU during Phase-II of transmission. The performance of FU is also better than NU. This improvement in performance is due to the higher power assigned to the FU as shown in (3) compared to the NU. It can be concluded from the figure that when comparing the BER versus SNR performance, cooperative NOMA outperforms conventional NOMA system.

Fig. 5 shows the comparison between the conventional NOMA over cooperative NOMA when data rate is compared with the power allocation of the system. It can be inferred from Fig. 5 that when FU and NU are deployed in conventional NOMA, the system requires 3.5 bits to transmit at 0.1 power allocation. This point is determined by observing the intersection point of FU and NU. Whereas when NU and FU are deployed in a cooperative NOMA model they need 1.5 bits to transmit at the same power allocation which means that cooperative NOMA system can utilize the bandwidth more effectively as compared to the conventional NOMA model. Finally, from this figure, the impact of cooperative NOMA can be observed that the FU with cooperation outperforms the FU without cooperation in terms of data rate.

Fig. 6 demonstrates the movement of the NU and FU from the BS. It can be observed that when FU and NU are very close to BS and thus allocating the same power level the performance of the system drops drastically as SIC is not able to decode the strong user accurately. Therefore, the performance significantly improves as the FU starts moving away from the BS. As the NU and FU are required to have the same decoded rate, more power is required to be applied at the symbol information (which is far away from BS) to significantly improve the performance of the cooperative model. Thus, it is recommended that when deploying FU and NU they are further apart from each other as indicated by the simulation results.

Fig. 7 presents the cooperative NOMA system when EXIT chart analysis is employed. Mutual Information (MI) is utilized by the inner decoder, while the channel decoding/despreading information is employed by the outer decoder, respectively. As the Spreading Factor (SF) is fixed to 2 and the $R = 1/2$, the joint spreading is equivalent to 0.25. From this figure, it can be easily observed that there is a loss initially as the both ones and zeros are initialized with the same probability of 0.5. It can be observed that the open tunnel exists around a given SNR of -10 dB. Therefore, if suitable number of iterations are employed between the

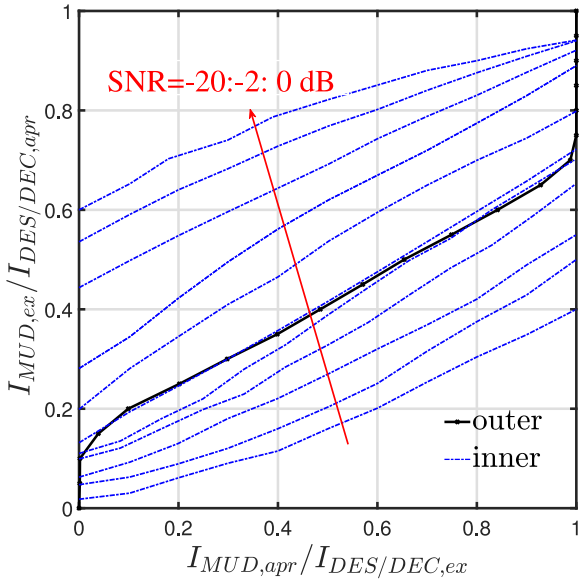

FIGURE 7. EXIT chart of a NOMA system, where the outer decoder operates with RSC code having $SF = 2$ when the inner decoder for various values of SNR are used in MUD model.

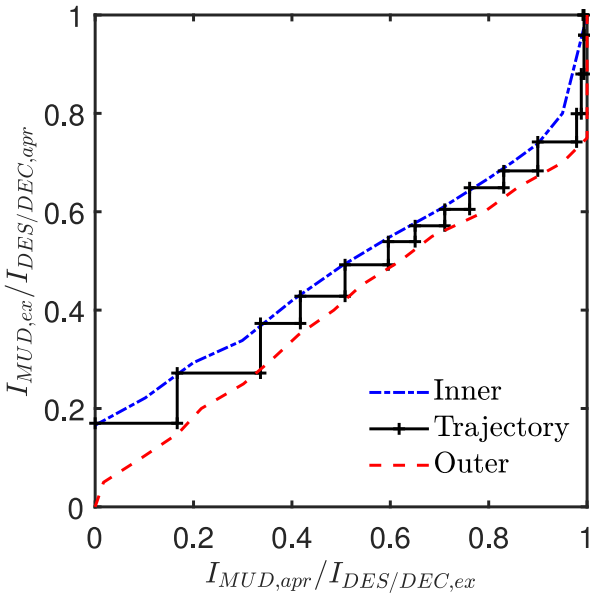

FIGURE 8. EXIT chart analysis by adopting the IRCC codes for NOMA system.

decoder and despreader, an error free transmission can occur. Finally, from this figure, it can be concluded that EXIT charts can be employed for cooperative NOMA provided suitable number of iterations are chosen between MUD_{DEC} and MUD_{DES}.

In order to analyst the capabilities of the MUD, a $SF = 2$ is utilized by exploiting the IRCC codes as shown in Fig. 8. It can be observed from Fig. 8 that a narrow path between the inner and outer curves exist in the EXIT chart at the $SNR = -10$ dB. An open tunnel is observed when the trajectory matches indicating that convergence of the system is achieved. This convergence point $[1, 1]$ is shown

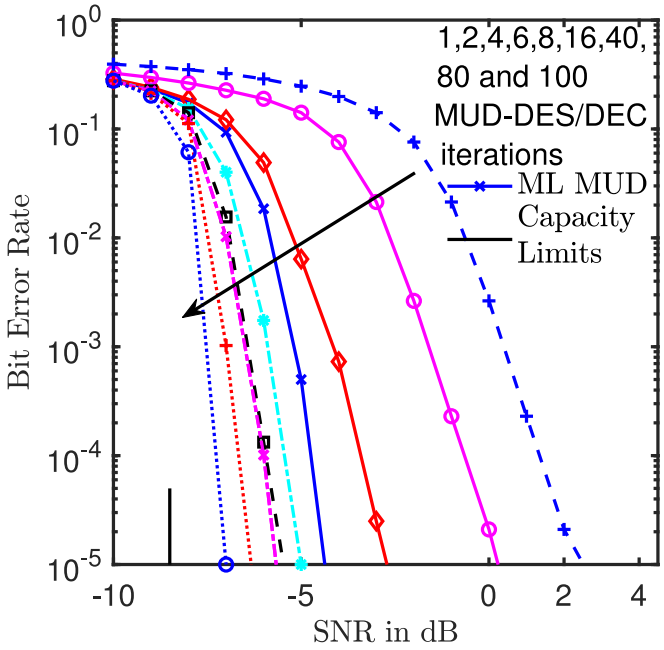

FIGURE 9. BER performance versus SNR for a MUD system, where various number of MUD DES/DEC iterations are utilized when SF=2.

at the right corner of Fig. 8. A Gaussian distribution is used in the MUD to calculate the *a priori* LLRs for the inner decoder, where the inner curve overshoot for the Maximum A Posteriori (MAP) for $0 < I_{MUD_{apr}} < 1$ as shown in Fig. 8. The outer curve of EXIT chart is produced by an IRCC, which matches to the MAP MUD's inner curve of EXIT chart as observed in Fig. 8. The outer curve rate is $R/SF = 0.4$ with $SF = 2$, where all users transmit on the available sub-carriers. We may observe that the decoding trajectory passes through the open tunnel of EXIT chart and converges at $I_{DES=DEC;ex} = 0.96$ after performing 1000 iterations between the $MUD_{DES/DEC}$ thus resulting in a vanishingly low BER.

The BER performance of the MUD system is presented in Fig. 9. It can be observed from Fig. 9 that after performing 100 decoding iterations, we are 1.08 dB away from Shannon channel capacity as indicated by the BER line at $= 10^{-5}$, where the SNR $= -8.68$ dB. This is because of two factors, firstly, the limited length of the interleaver, i.e., 2048 bits per user and secondly due to the outer code, which does not reach the $I_{DES=DEC;ex} = 1$ line in Fig. 9. It can be concluded that by performing more than 100 iterations we might achieve optimal performance of Shannon capacity which indicates that our proposed model can perform better if more decoding iterations can be done in the MUD model.

V. CONCLUSION

NOMA based cooperative relaying was shown, through our simulations, to achieve significantly improved performance for the proposed system. User Fairness was also shown to be at near-optimal performance through our utilization of EXIT charts. This is due to the inner and outer curves of the EXIT charts converging towards unity gain without any

intersection at any point beforehand. Furthermore, our MUD approach with the implementation of IRCC coding was illustrated through the use of EXIT charts and was shown to offer flexibility in the coding rate which increases overall throughput efficiency, thereby, a design methodology for combining SISO MUD with IRCC is presented. The reduction of computational complexity in terms of EXIT curves was the main reason for choosing IRCC as well as its prospective ability to attain near peak performance. The benefits of embracing cooperative relaying are made clear by utilizing EXIT charts. As a result, the proposed NOMA system model can be applied in cooperative networks to strike a balance between user fairness and user data rates. Expanding the proposed cooperative NOMA system to function in a MIMO scenario by incorporating user fairness at a practical level will be a promising future direction of research.

REFERENCES

[1] B. Makki, K. Chitti, A. Behravan, and M.-S. Alouini, "A survey of NOMA: Current status and open research challenges," *IEEE Open J. Commun. Soc.*, vol. 1, pp. 179–189, 2020.

[2] M. Elbayoumi, M. Kamel, W. Hamouda, and A. Youssef, "NOMA-assisted machine-type communications in UDN: State-of-the-art and challenges," *IEEE Commun. Surveys Tuts.*, vol. 22, no. 2, pp. 1276–1304, 2nd Quart., 2020.

[3] M. Vaezi, R. Schober, Z. Ding, and H. V. Poor, "Non-orthogonal multiple access: Common myths and critical questions," *IEEE Wireless Commun.*, vol. 26, no. 5, pp. 174–180, Oct. 2019.

[4] Z. Ding *et al.*, "Application of non-orthogonal multiple access in LTE and 5G networks," *IEEE Commun. Mag.*, vol. 55, no. 2, pp. 185–191, Feb. 2017.

[5] Y. Liu, Z. Qin, M. Elkashlan, Z. Ding, A. Nallanathan, and L. Hanzo, "Nonorthogonal multiple access for 5G and beyond," *Proc. IEEE*, vol. 105, no. 12, pp. 2347–2381, Dec. 2017.

[6] L. Chettri and R. Bera, "A comprehensive survey on Internet of Things (IoT) toward 5G wireless systems," *IEEE Internet Things J.*, vol. 7, no. 1, pp. 16–32, Jan. 2020.

[7] Q. Z. Ahmed, M. Hafeez, F. A. Khan, and P. Lazaridis, "Towards beyond 5G future wireless networks with focus towards indoor localization," in *Proc. IEEE 8th Int. Conf. Commun. Netw. (ComNet)*, 2020, pp. 1–5.

[8] E. H. G. Yousif, M. C. Filippou, F. Khan, T. Ratnarajah, and M. Sellathurai, "A new LSA-based approach for spectral coexistence of MIMO radar and wireless communications systems," in *Proc. IEEE Int. Conf. Commun. (ICC)*, 2016, pp. 1–6.

[9] S. M. R. Islam, N. Avazov, O. A. Dobre, and K. Kwak, "Power-domain non-orthogonal multiple access (NOMA) in 5G systems: Potentials and challenges," *IEEE Commun. Surveys Tuts.*, vol. 19, no. 2, pp. 721–742, 2nd Quart., 2017.

[10] Z. Chen, Z. Ding, X. Dai, and R. Zhang, "An optimization perspective of the superiority of NOMA compared to conventional OMA," *IEEE Trans. Signal Process.*, vol. 65, no. 19, pp. 5191–5202, Oct. 2017.

[11] O. Alluhaibi, Q. Z. Ahmed, E. Kampert, M. D. Higgins, and J. Wang, "Revisiting the energy-efficient hybrid DA precoding and combining design for mm-Wave systems," *IEEE Trans. Green Commun. Netw.*, vol. 4, no. 2, pp. 340–354, Jun. 2020.

[12] A. S. de Sena *et al.*, "Massive MIMO-NOMA networks with imperfect SIC: Design and fairness enhancement," *IEEE Trans. Wireless Commun.*, vol. 19, no. 9, pp. 6100–6115, Sep. 2020.

[13] G. K. Papageorgiou *et al.*, "Advanced dynamic spectrum 5G mobile networks employing licensed shared access," *IEEE Commun. Mag.*, vol. 58, no. 7, pp. 21–27, Jul. 2020.

[14] Y. He, J. Xue, T. Ratnarajah, M. Sellathurai, and F. Khan, "On the performance of cooperative spectrum sensing in random cognitive radio networks," *IEEE Syst. J.*, vol. 12, no. 1, pp. 881–892, Mar. 2018.

[15] L. Dai, B. Wang, Y. Yuan, S. Han, I. Chih-Lin, and Z. Wang, "Non-orthogonal multiple access for 5G: Solutions, challenges, opportunities, and future research trends," *IEEE Commun. Mag.*, vol. 53, no. 9, pp. 74–81, Sep. 2015.

[16] B. Wang, L. Dai, Z. Wang, N. Ge, and S. Zhou, "Spectrum and energy-efficient beamspace MIMO-NOMA for millimeter-wave communications using lens antenna array," *IEEE J. Sel. Areas Commun.*, vol. 35, no. 10, pp. 2370–2382, Oct. 2017.

[17] Z. Xiao, L. Zhu, Z. Gao, D. O. Wu, and X. Xia, "User fairness non-orthogonal multiple access (NOMA) for millimeter-wave communications with analog beamforming," *IEEE Trans. Wireless Commun.*, vol. 18, no. 7, pp. 3411–3423, Jul. 2019.

[18] Y. Liu, Z. Ding, M. Elkashlan, and J. Yuan, "Nonorthogonal multiple access in large-scale underlay cognitive radio networks," *IEEE Trans. Veh. Technol.*, vol. 65, no. 12, pp. 10152–10157, Dec. 2016.

[19] P. K. Sangdeh, H. Pirayesh, Q. Yan, K. Zeng, W. Lou, and H. Zeng, "A practical downlink NOMA scheme for wireless LANs," *IEEE Trans. Commun.*, vol. 68, no. 4, pp. 2236–2250, Apr. 2020.

[20] M. Vaezi, G. A. A. Baduge, Y. Liu, A. Arafa, F. Fang, and Z. Ding, "Interplay between NOMA and other emerging technologies: A survey," *IEEE Trans. Cogn. Commun. Netw.*, vol. 5, no. 4, pp. 900–919, Dec. 2019.

[21] F. Zhou, Y. Wu, Y.-C. Liang, Z. Li, Y. Wang, and K.-K. Wong, "State of the art, taxonomy, and open issues on cognitive radio networks with NOMA," *IEEE Wireless Commun.*, vol. 25, no. 2, pp. 100–108, Apr. 2018.

[22] L. Dai, B. Wang, Z. Ding, Z. Wang, S. Chen, and L. Hanzo, "A survey of non-orthogonal multiple access for 5G," *IEEE Commun. Surveys Tuts.*, vol. 20, no. 3, pp. 2294–2323, 3rd Quart., 2018.

[23] Z. Ding, M. Peng, and H. V. Poor, "Cooperative non-orthogonal multiple access in 5G systems," *IEEE Commun. Lett.*, vol. 19, no. 8, pp. 1462–1465, Aug. 2015.

[24] M. Moltafet, N. M. Yamchi, M. R. Javan, and P. Azmi, "Comparison study between PD-NOMA and SCMA," *IEEE Trans. Veh. Technol.*, vol. 67, no. 2, pp. 1830–1834, Feb. 2018.

[25] Z. Ding, Z. Yang, P. Fan, and H. V. Poor, "On the performance of non-orthogonal multiple access in 5G systems with randomly deployed users," *IEEE Signal Process. Lett.*, vol. 21, no. 12, pp. 1501–1505, Dec. 2014.

[26] Z. Ding, X. Lei, G. K. Karagiannidis, R. Schober, J. Yuan, and V. K. Bhargava, "A survey on non-orthogonal multiple access for 5G networks: Research challenges and future trends," *IEEE J. Sel. Areas Commun.*, vol. 35, no. 10, pp. 2181–2195, Oct. 2017.

[27] S. Riaz, F. A. Khan, S. Saleem, and Q. Z. Ahmed, "Reducing the mutual outage probability of cooperative non-orthogonal multiple access," *IEEE Trans. Veh. Technol.*, vol. 69, no. 12, pp. 16207–16212, Dec. 2020.

[28] Y. Liu, Z. Qin, M. Elkashlan, Y. Gao, and L. Hanzo, "Enhancing the physical layer security of non-orthogonal multiple access in large-scale networks," *IEEE Trans. Wireless Commun.*, vol. 16, no. 3, pp. 1656–1672, Mar. 2017.

[29] Z. Elsaraf, A. Ahmed, F. A. Khan, and Q. Z. Ahmed, "EXIT chart analysis of cooperative non-orthogonal multiple access for next generation wireless communication systems," in *Proc. Eur. Conf. Netw. Commun. (EuCNC)*, 2020, pp. 281–285.

[30] G. Liu, X. Chen, Z. Ding, Z. Ma, and F. R. Yu, "Hybrid half-duplex/full-duplex cooperative non-orthogonal multiple access with transmit power adaptation," *IEEE Trans. Wireless Commun.*, vol. 17, no. 1, pp. 506–519, Jan. 2018.

[31] D. Wan, M. Wen, F. Ji, H. Yu, and F. Chen, "Non-orthogonal multiple access for cooperative communications: Challenges, opportunities, and trends," *IEEE Wireless Commun.*, vol. 25, no. 2, pp. 109–117, Apr. 2018.

[32] Z. Yang, Z. Ding, Y. Wu, and P. Fan, "Novel relay selection strategies for cooperative NOMA," *IEEE Trans. Veh. Technol.*, vol. 66, no. 11, pp. 10114–10123, Nov. 2017.

[33] D. Wan, M. Wen, X. Cheng, S. Mumtaz, and M. Guizani, "A promising non-orthogonal multiple access based networking architecture: Motivation, conception, and evolution," *IEEE Wireless Commun.*, vol. 26, no. 5, pp. 152–159, Oct. 2019.

[34] M. F. Kader, M. B. Shahab, and S. Y. Shin, "Exploiting non-orthogonal multiple access in cooperative relay sharing," *IEEE Commun. Lett.*, vol. 21, no. 5, pp. 1159–1162, May 2017.

[35] L. Lv, J. Chen, Q. Ni, Z. Ding, and H. Jiang, "Cognitive non-orthogonal multiple access with cooperative relaying: A new wireless Frontier for 5G spectrum sharing," *IEEE Commun. Mag.*, vol. 56, no. 4, pp. 188–195, Apr. 2018.

[36] L. Lv, J. Chen, Q. Ni, and Z. Ding, "Design of cooperative non-orthogonal multicast cognitive multiple access for 5G systems: User scheduling and performance analysis," *IEEE Trans. Commun.*, vol. 65, no. 6, pp. 2641–2656, Jun. 2017.
[37] C. Zhong and Z. Zhang, "Non-orthogonal multiple access with cooperative full-duplex relaying," *IEEE Commun. Lett.*, vol. 20, no. 12, pp. 2478–2481, Dec. 2016.
[38] K. Singh, K. Wang, S. Biswas, Z. Ding, F. A. Khan, and T. Ratnarajah, "Resource optimization in full duplex non-orthogonal multiple access systems," *IEEE Trans. Wireless Commun.*, vol. 18, no. 9, pp. 4312–4325, Sep. 2019.
[39] M. B. Shahab, M. F. Kader, and S. Y. Shin, "A virtual user pairing scheme to optimally utilize the spectrum of unpaired users in non-orthogonal multiple access," *IEEE Signal Process. Lett.*, vol. 23, no. 12, pp. 1766–1770, Dec. 2016.
[40] M. B. Shahab and S. Y. Shin, "A time sharing based approach to accommodate similar gain users in NOMA for 5G networks," in *Proc. IEEE 42nd Conf. Local Comput. Netw. Workshops (LCN Workshops)*, 2017, pp. 142–147.
[41] Y. Ge, Q. Deng, P. C. Ching, and Z. Ding, "OTFS signaling for uplink NOMA of heterogeneous mobility users," *IEEE Trans. Commun.*, early access, Feb. 15, 2021, doi: 10.1109/TCOMM.2021.3059456.
[42] S. ten Brink, "Designing iterative decoding schemes with the extrinsic information transfer chart," *AEU Int. J. Electron. Commun.*, vol. 54, no. 6, pp. 389–398, 2000.
[43] M. El-Hajjar and L. Hanzo, "EXIT charts for system design and analysis," *IEEE Commun. Surveys Tuts.*, vol. 16, no. 1, pp. 127–153, 1st Quart., 2014.
[44] S. Sugiura, S. Chen, and L. Hanzo, "Coherent and differential space-time shift keying: A dispersion matrix approach," *IEEE Trans. Commun.*, vol. 58, no. 11, pp. 3219–3230, Nov. 2010.
[45] A. Ahmed, P. Botsinis, S. Won, L. Yang, and L. Hanzo, "EXIT chart aided convergence analysis of recursive soft *m*-sequence initial acquisition in Nakagami-*m* fading channels," *IEEE Trans. Veh. Technol.*, vol. 67, no. 5, pp. 4655–4660, May 2018.
[46] A. Ahmed, P. Botsinis, S. Won, L. Yang, and L. Hanzo, "Primitive polynomials for iterative recursive soft sequential acquisition of concatenated sequences," *IEEE Access*, vol. 7, pp. 13882–13900, 2019.
[47] L. Hanzo, T. H. Liew, B. L. Yeap, R. Y. S. Tee, and S. X. Ng, *Turbocoded Adaptive Modulation versus Spacetime Trellis Codes for Transmission over Dispersive Channels*. Hoboken, NJ, USA: Wiley, 2011, pp. 233–252.
[48] S. Sugiura and L. Hanzo, "Single-RF spatial modulation requires single-carrier transmission: Frequency-domain turbo equalization for dispersive channels," *IEEE Trans. Veh. Technol.*, vol. 64, no. 10, pp. 4870–4875, Oct. 2015.

ABBAS AHMED received the B.E.E. degree in electrical engineering (specialization in electronics) from Air University, Islamabad, Pakistan, in 2007, the M.Sc. degree (Distinction) from the University of Southampton, U.K., in 2009, and the Ph.D. degree in electronics and electrical engineering from the University of Southampton in 2019. During the Ph.D., he worked on synchronization issues for the wireless communication system and designed diverse algorithms by using iterative decoding for synchronization. He is currently working as a Postdoctoral Research Assistant with the University of Huddersfield, U.K. His major research interests in wireless communication are initial synchronization, iterative detection, device to device communications, cooperative communication, non-orthogonal multiple access techniques, EXIT chart analysis, and fast frequency hopping system.

ZEYAD ELSARAF received the B.Eng. degree (Hons., High Distinction) from the University of Huddersfield, Huddersfield, U.K., in 2017, and the master's degree in computer game design from the University of Essex, U.K., in 2018. He is currently pursuing the Ph.D. degree in electric and electronic engineering with the University of Huddersfield. His research interests include wireless technology aimed toward 5G and beyond cellular networks with a focus on non-orthogonal multiple access techniques. He was a recipient of the Chancellor's Award for outstanding achievement by an undergraduate engineering student from the University of Huddersfield.

FAHEEM A. KHAN (Member, IEEE) received the Ph.D. degree in electrical and electronic engineering from Queen's University Belfast, U.K., in 2012. He worked as a Lecturer of Electronic Engineering with the Higher Colleges of Technology, UAE, from 2012 to 2014. In 2014, he joined as a Research Associate of Wireless Communications and Signal Processing with the Institute for Digital Communications, University of Edinburgh, U.K. From 2016 to 2018, he was a Lecturer of Electronic Engineering with the School of Computing and Engineering, University of Huddersfield, U.K., where he has been a Senior Lecturer since 2018. His current research interests include spectrum sharing for beyond 5G wireless networks, licensed shared access and cognitive radio, non-orthogonal multiple access, machine learning and deep learning in wireless communications, full-duplex communications, MIMO communications, millimeter wave communications, and Internet of Things networks. He is currently a Co-Investigator of EU H2020 ETN Research Project "MObility and Training fOR beyond 5G Ecosystems (MOTOR5G)," and EU H2020 RISE Research Project "Research Collaboration and Mobility for Beyond 5G Future Wireless Networks (RECOMBINE)." He is a Fellow of Higher Education Academy (FHEA).

QASIM ZEESHAN AHMED received the Ph.D. degree from the University of Southampton, Southampton, U.K., in 2009. He worked as an Assistant Professor with the National University of Computer and Emerging Sciences (NUCES-FAST) Islamabad, Pakistan, from November 2009 to June 2011. He has been a Postdoctoral Fellow with the Computer, Electrical and Mathematical Sciences and Engineering Division, King Abdullah University of Science and Technology, Thuwal, Saudi Arabia, from June 2011 to June 2014. He joined the University of Kent, U.K., as a Lecturer from January 2015 to January 2017. He was a Lecturer, then a Senior Lecturer, and currently a Reader of Electronic Engineering with the School of Computing and Engineering, University of Huddersfield, U.K., in 2017, 2018, and 2020, respectively. His research interests include mainly ultrawide bandwidth systems, millimeter waves, device to device, digital health, and cooperative communications. He is currently a Principal Investigator for Erasmus + Project "Capacity Building for Health Monitoring and Care Systems, DigiHealth-Asia," a Co-Investigator of EU H2020 ETN Research Project "MObility and Training fOR beyond 5G Ecosystems (MOTOR5G)," and EU H2020 RISE Research Project "Research Collaboration and Mobility for Beyond 5G Future Wireless Networks (RECOMBINE)." He is a Fellow of Higher Education Academy (FHEA).